Engineering Structures 107 (2016) 23–33

Contents lists available at ScienceDirect

Engineering Structures

journal homepage: www.elsevier.com/locate/engstruct

The influence of reinforcement on load carrying capacity and cracking of the reinforced concrete deep beam joint

Anna Kopańska *, Krystyna Nagrodzka-Godycka

Department of Concrete Structures, Gdansk University of Technology, Gdansk, Poland

ARTICLE INFO

Article history:
Received 19 February 2015
Revised 28 October 2015
Accepted 2 November 2015
Available online 18 November 2015

Keywords:
Deep beams
Cantilevers
Reinforced concrete
Cracks
Load carrying capacity
Strut-and-Tie model
Softening coefficient

ABSTRACT

The paper presents the results of experimental research of the spatial reinforced concrete deep beam systems orthogonally reinforced and with additional inclined bars. Joint of the deep beams in this research was composed of the longitudinal deep beam with a cantilever suspended at the transversal deep beam. The cantilever deep beam was loaded throughout the depth and the transversal deep beam was loaded at the mid-span by longitudinal deep beam attached to it. Morphology of cracking and stresses in the reinforcing steel, as well as the load distribution in the cantilever deep beams using Strut-and-Tie model taking into account an effort of concrete compression strut and efficiency of softening coefficient are presented and discussed. In the paper, the effectiveness of the mixed reinforcement in both tested deep beam systems, as referred to the design recommendation proposed in the published papers is also verified. It is also demonstrated that the inclined reinforcement favorably influences the width of cracks in cantilever and transversal deep beams and ensures the increase of the load carrying capacity.

© 2015 Published by Elsevier Ltd.

1. Introduction

In recent years, we can observed a major increase in the number of high-rise buildings especially in the large cities, where the demand is often associated with a lack of available land. Therefore importance of design reinforced concrete deep beams significantly increased as main structural elements in this type of structures (Fig. 1). Seeking the more attractive architectural forms of buildings, the unusual special shape of the building's body, as well as diversified facades are looked for. In such cases, the deep beams are the essential structural elements. They are applied in order to break the monotony of smooth walls with the help of jutties (bays) thus creating special deep beam joints with the elements of cantilever deep beams.

The loading applied on particular deep beams, cantilever ones included, produce stress state and cracks different from flat deep beams that are tested most frequently. The standard regulations, both EC 2 [1], and ACI 318 [2], or MC 2010 [3], do not consider cantilever and transversal deep beams loaded along their depth.

The extensive experimental research of concrete reinforced deep beams conducted so far, in a large majority concerned the load carrying capacity of flat deep beams, single or twin span loaded with forces concentrated on the upper edge with unbounded edges [4–6], or suspended to the columns [7]. The variable parameters were diversified in those tests and concerned, i.a., reinforcement [8–10], various deep beams geometry [11,12], and the influence of the concrete strength [13].

The tests of the spatial system of deep beams where the cantilever deep beam was an element of system loaded along the upper edge, were conducted in the 60th of the XX century by Leonhardt [14] and Walther [15]. On the basis of obtained results, Leonhardt formulated the design recommendations, concerning i.a. the cantilever elements loaded indirectly along the depth, that are applied till today.

2. The state of knowledge regarding the actual design recommendations

The Leonhard's [14] recommendations regarding the cantilever deep beams uniformly loaded along depth are based on the assumption that vertical bars in the form of stirrups, concentrated near the edge of the cantilever are to be dimensioned for the force of $0.6F$, while the bent up bars should be dimensioned for the force of $0.4F_1/\sin\alpha$ as in Fig. 2.

$$A_{sw1} = 0.6 \cdot \frac{F_1}{f_{ywd}} \tag{1}$$

* Corresponding author.
E-mail addresses: anna.kopanska@pg.gda.pl (A. Kopańska), ngodyc@pg.gda.pl (K. Nagrodzka-Godycka).

http://dx.doi.org/10.1016/j.engstruct.2015.11.001
0141-0296/© 2015 Published by Elsevier Ltd.

Downloaded from http://www.elearnica.ir

Nomenclature

a_F	dimension the force from the edge of the cantilever deep beam
A_{sw1}	area of the vertical bars
A_{sw2}	area of the bent up bars
d	effective height of the cantilever deep beam
E_c	Young modulus of concrete
f_c	compressive strength
$f_{cm,cyl}$	cylinder compressive strength of concrete
f_y	yield strength of the reinforcement
F	total applied force acting on the deep beam system
F_1	force distributed throughout the depth of the cantilever deep beam
F_3	force transmitted to the transversal deep beam along its depth
$F_{c1,cal}$, $F_{c2,cal}$	compressive force of concrete in the strut from the analysis S–T
$F_{s1,cal}$, $F_{s2,cal}$	tensile force of reinforcement from the analysis S–T
$F_{s1,exp}$, $F_{s2,exp}$	tensile force of reinforcement from the exp. tests
F_{cr}	cracking force
F_t	force in diagonal reinforcement
F_u	failure load
$F_{u,design}$	designed failure load
F_v	force in vertical reinforcement
H	height of the deep beam
l_k	overhang length of the cantilever deep beam
t	thickness of the deep beam
u	vertical displacement of the bottom horizontal edge at the end of the cantilever deep beam
w_i	width of the cracks
α	angle between the bent up bars and the horizontal axis
α_2	angle between the force F_{s2} and the vertical axis
β	softening coefficient
ε_c	compressive strain in the concrete
ε_{ct}	tensile strain in the concrete
θ	angle between the force F_{c1} and F_{s1}
$\sigma_{c1,cal}$, $\sigma_{c2,cal}$	compressive stresses of concrete in the strut from the analysis
$\sigma_{s,exp}$	stresses of the main reinforcement from the exp. tests

Fig. 1. High-rise buildings and building due to architectural reasons.

$$A_{sw2} = 0.4 \cdot \frac{F_1}{\sin\alpha \cdot f_{ywd}} \tag{2}$$

The vertical bars shaped as a stirrup closed at the whole depth of the deep beam, transmitting the force $0.6F$, are to be disposed in the transversal beam on the $2t$ section from its edge.

The suggestions recommended by Schröeder's [16] are different. He proposes that the bent up bars take over the entire force acting on the cantilever F_1, and that the additional vertical stirrups dimensioned for the force of $0.4F$ are placed. These recommendations do not take into account angle of inclined bars according to span–depth ratio (see Fig. 3).

$$A_{sw1} = 0.4 \cdot \frac{F_1}{f_{ywd}} \tag{3}$$

$$A_{sw2} = \frac{F_1}{f_{ywd}} \tag{4}$$

In the case of the reinforcement of a simple-supported deep beam, on which another deep beam is attached along its whole height, Leonhardt [14] recommends to introduce the additional reinforcement in the form of stirrups, or the reinforcement in the form of vertical stirrups and bent up bars of bending diameter equal to 20ϕ. While the vertical reinforcement is applied at the deep beams joint, the stirrups transmitting the entire force F should be situated along the width of $3t$ nearly the joint [16] (Fig. 4).

3. The importance of the research

In order to experimentally determine the effectiveness of diagonal reinforcement according to Leonhardt's [14] recommendations of, as well as to check up of application of the orthogonal reinforcement only, in the case of a joint with the cantilever deep beam loaded at its depth, the original research of two spatial deep beam systems was carried on. For the analysis of the flow of forces

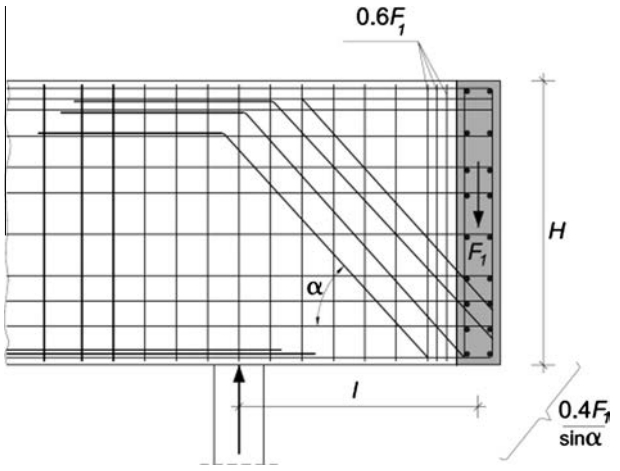

Fig. 2. Reinforcement of a cantilever deep beam according to Leonhardt [14].

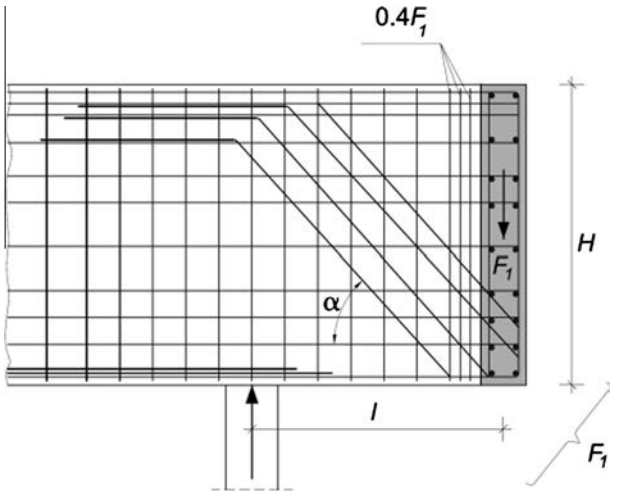

Fig. 3. Reinforcement of a cantilever deep beam according to Schroeder [16].

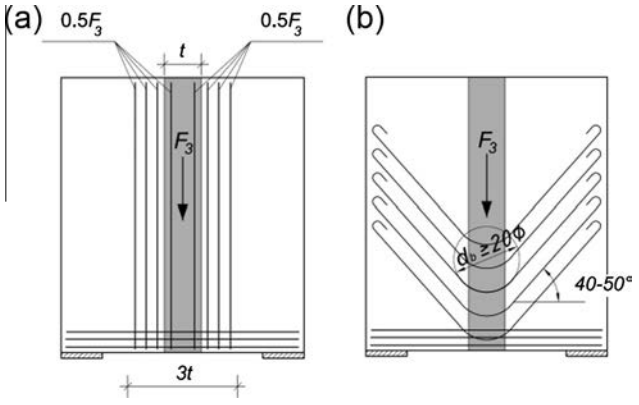

Fig. 4. Reinforcement in the transversal deep beam related to: (a) vertical stirrups [16]; and (b) bent up bars [14].

in the cantilever deep beams loaded throughout the depth also adopted a model Strut and Tie include an effort of concrete compression strut and efficiency of softening coefficient. The deep beam joint in this research was composed of the longitudinal deep beam with a cantilever suspended at the transversal deep beam. The cantilever deep beam was loaded throughout the depth. In the transversal deep beam the load at the mid-span was longitudinal deep beam attached to it. In the paper, the results of experimental tests of the spatial system of two cantilever and transversal deep beams are presented: orthogonally reinforced DBI and the other DBII with additional diagonal bars. The results of the tests are compared with the recommendations of construction of reinforcement existing in the published papers [14,16].

4. Experimental program

4.1. Specimen details

The tests were conducted for the spatial system of joints of two reinforced concrete deep beams of identical geometry and different reinforcement. They were composed of longitudinal deep beams with a cantilever of the ratio $l_k/H = 0.5$ hanged over the transversal deep beam with corner supports at the bottom. The deep beam were 100 mm thick and 1000 mm high. In Fig. 5, the geometry of the deep beam joints DBI and DBII and the scheme of loading on the test stand are presented.

The program of the research consisted of two deep beam systems with different reinforcement, the DBI orthogonally reinforced, and the DBII with additional diagonal bars. The spatial deep beam system was reinforced with bars of diameter 8, 10, and 12 mm (Figs. 6 and 7). The reinforcement as it concerns the strength and the spatial arrangement was adopted on the base of the analysis of the state of stress of a deep beam system, in connection with constructional recommendations [14], assumed the overall vertical loading $F = 1200$ kN. In the area of the supports of the transversal deep beams, an additional reinforcement for bearing stress in the form of welded up grids of 6 mm diameter in three layers was applied.

The system of deep beams were concreted in vertical position applying the self-compacting concrete mix of the mean compressive strength of $f_{cm,cyl} = 50$ MPa tested on ten cylindrical specimens 150/300 mm and was measured during the testing deep beams. The yield strength of the main reinforcement bars was $f_y = 582$ MPa for bars of Ø8 mm, and $f_y = 534$ MPa for bars of Ø10 mm, and $f_y = 556$ MPa for bars of Ø12 mm [17].

4.2. The set-up

In order to transmit the load to the part of the reinforced deep beam: span and cantilever ones throughout the depth, a special set-up was arranged and adopted to the hydraulic testing machine Walter + Bai A.G. of 5000 kN capacity (Figs. 8 and 9).

The deep beam system was loaded with the final force F which through the steel traverses was transmitted as two concentrated forces ($0.29F$ each) in the span to the upper edge, and force $F_1 = 0.42F$ distributed throughout the depth of cantilever. The force was transmitted to the cantilever deep beam by steel channel profile and horizontal bolts ϕ20 mm situated on the depth of the cantilever. The force of $F_3 = 0.92F$ was transmitted to the transversal deep beam along its depth with reaction equal to $0.46F$ (Fig. 8). At the end of the one-span cantilever deep beam the reaction, according to the distribution of forces was equal to $0.08F$ (Figs. 5 and 8).

4.3. The testing procedure

The test was carried out under displacement controlled load with a strain rate of 0.6 mm/min until the failure. During the loading, measurement of concrete and steel reinforcement strains, as well as of the displacements and width of cracks were carried on.

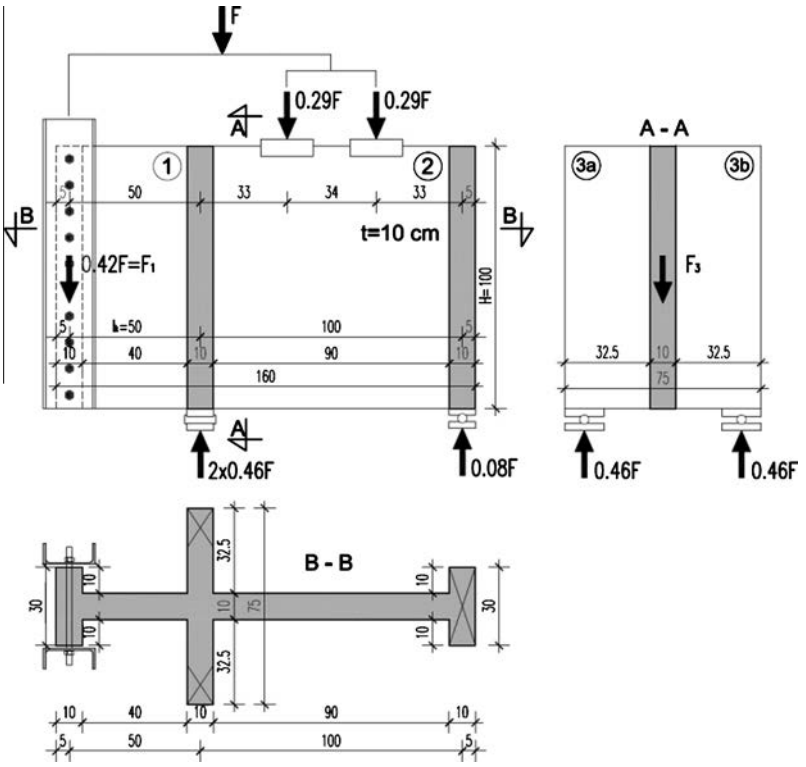

Fig. 5. Geometry, dimensions and scheme of loading of the DBI and DBII deep beams (unit: cm).

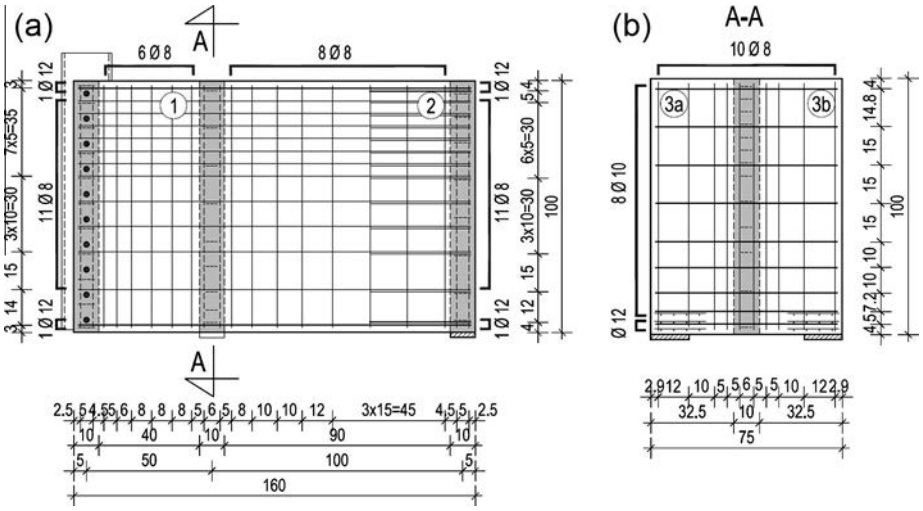

Fig. 6. The reinforcement of the DBI: (a) longitudinal deep beam with cantilever, and (b) transversal deep beam.

The strains of reinforcement steel were measured using the foil electrical resistance strain gauges (Vishay EA-06 240LZ_120/E with a length of 10 mm, the basis of measurement of 6.1 mm a resistance equal to 120 Ω ± 0.3%) while concrete strains were measured on the surface of the deep beam using the mechanical extensometer with 100 mm basis. (This device allows measurements of up to 0.001 mm corresponding to the unit value of deformation $0.805 * 10^{-5}$.) For measuring the crack width, a microscope with a magnification of 40× was used. The measurement of the horizontal edge of deep beams displacement was made with an inductive sensors (LVDT).

5. Experimental results

Due to the non-linear distribution of stresses in the reinforced concrete deep beams, the most appropriate for the design of such structural elements is a model Strut-and-Tie or nonlinear analysis. Strut-and-Tie model analysis of reinforced concrete elements is considered an alternative to the usual approaches of analysis and design, and is applied effectively in regions of discontinuity. In the previous literature, we find a lot of interesting scientific publications relating to the analysis of the load carrying capacity of deep beams with single or twin span using the S–T model and the theory

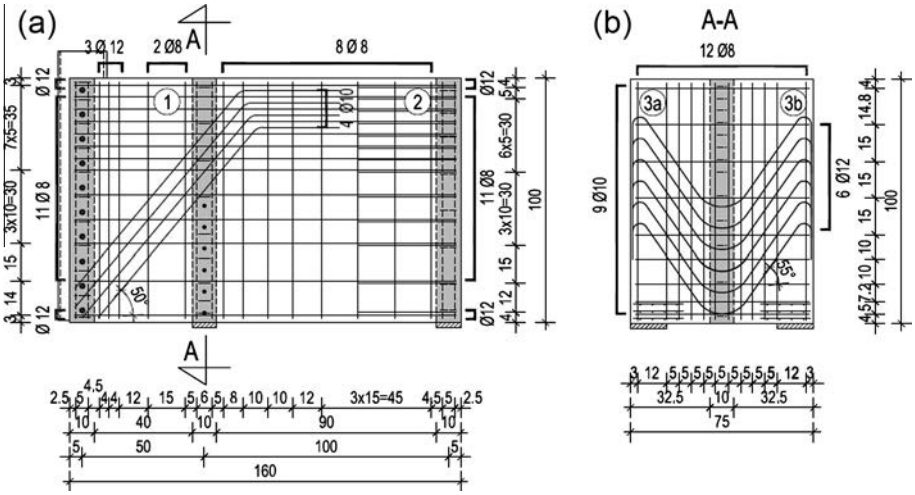

Fig. 7. The reinforcement of the DBII: (a) longitudinal deep beam with cantilever, and (b) transversal deep beam.

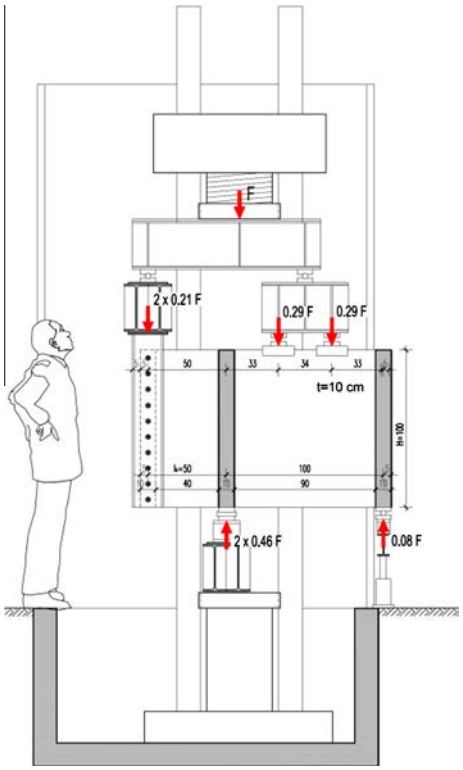

Fig. 8. Test set-up.

Fig. 9. Test set-up of DBI deep beams.

of stress fields [19–22]. The comparison S–T model with analysis of nonlinear finite element method of Vollum's [23] for deep beams with single and twin span is definitely worth attention.

In the presented analysis, distribution of load in the deep beams DBI and DBII based on the measured strains of steel and concrete obtained from own experimental tests and analytical using Strut-and-Tie model was determined. The study analyzed the flow of forces in the cantilever and transversal deep beams in relation to the recommendations by [15,16], in which assumptions are based on the setting the force resistance limits in the reinforcement using the S–T model. Additionally, the S–T model for corbels loaded throughout the depth according to Nagrodzka-Godycka [24] was also verified.

5.1. The flow of forces in a deep beam

In the diagrams (Figs. 10 and 11), the strains in the main steel reinforcement in both cantilever deep beams, together with a location of gauges arrangement, were shown. To calculate the stresses of steel used the average modulus of elasticity of steel E_s = 200 GPa on the basis of the Certificate of Material Properties. Based on the extensometer measurements of strains, the essential differences in the reinforcement strains distribution between the deep beams DBI and DBII may be noticed.

In the orthogonally reinforced cantilever, the vertical reinforcement bars reached locally the yielded (gauge No. 31) in the area of the external edge, while in the other measurement points, the strains of vertical bars were about ε_s = 1.5‰ (300 MPa ~0.5 f_y). In the DBII deep beam in the suspended vertical reinforcement, the average strains at the failure reached the value of appr. ε_s = 0.95‰ (180 MPa ~0.33f_y) and for the bent up bars ε_s = 2.0‰ (400 MPa ~0.75f_y) [17].

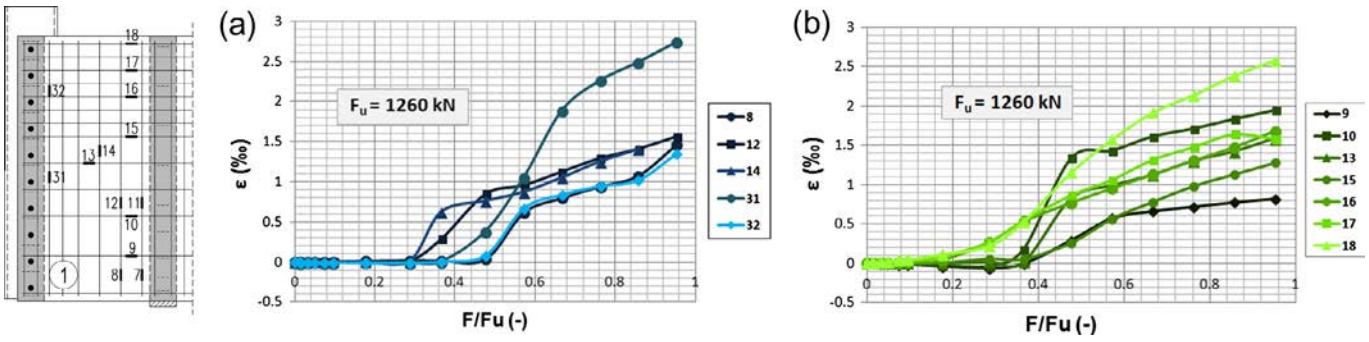

Fig. 10. Strains of the main reinforcement of the cantilever deep beam of DBI with the orthogonal reinforcement: (a) in vertical reinforcement, and (b) in horizontal reinforcement.

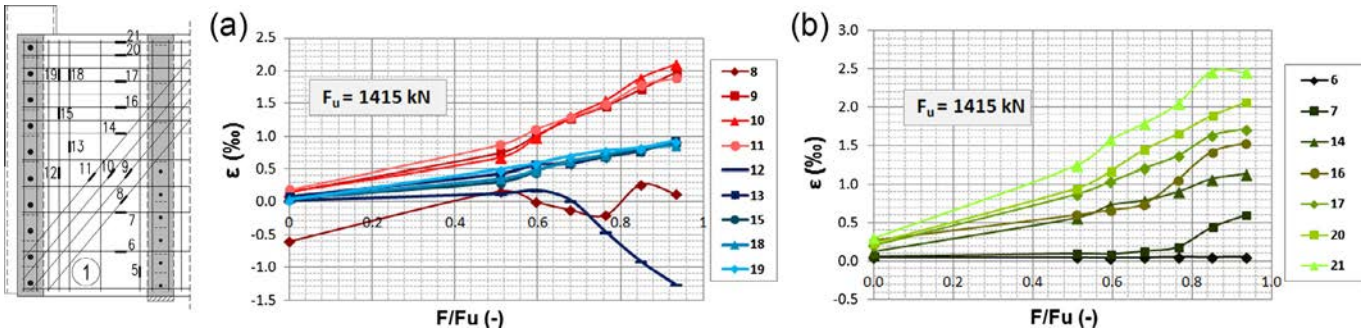

Fig. 11. Strains of the main reinforcement of the cantilever deep beam DBII with additional bent up bars: (a) in vertical and diagonal reinforcement, and (b) in horizontal reinforcement.

Table 1
Distribution of F_1 loading in the cantilever deep beam DBII for vertical reinforcement F_v and bent up one F_t.

Type of analysis	F_v (kN)	F_t (kN)	$F_t^* \sin a$ (kN)	F_1 (kN)	F_v/F (–)	$(F_t^* \sin a)/F_1$ (–)
From the exp. tests (8 bars[a], $\sigma_{s,exp}$)	123.1	250.2	191.7	314.8	0.40	0.60
From the exp. tests (6 bars[b], $\sigma_{s,exp}$)	123.1	187.7	143.8	266.9	0.46	0.54
Assuming $\sigma_{s,exp} = f_y$, 8 bars[a]	377.3	335.5	257.0	634.3	0.60	0.40
Assuming $\sigma_{s,exp} = f_y$, 6 bars[b]	377.3	251.6	192.8	570.1	0.66	0.34
According to [14] (for $F_{1,exp}$)	188.9	164.4	125.9	314.8	0.60	0.40
According to [16] (for $F_{1,exp}$)	125.9	410.9	314.8	314.8	0.40	1.00
Failure force from the statical analysis, $F = F_u$ = 1415 kN	–	–	–	594.3	–	–

[a] In the diagonal reinforcement from gauge No. 8, the mean stress as for remaining gauges was adopted.
[b] Reinforcement with gauge No. 8 was ignored according to Fig. 11.

In the vertical suspended reinforcement, in the case of the DBI, the steel strains reached higher value in the central part of the cantilever. In the DBII, the strains in vertical bars were of similar values along the whole depth of the cantilever, while the majority of loading was transmitted to the bent up bars.

In both cantilevers DBI and DBII, the stresses of horizontal reinforcement bars at the upper cantilevers edges were close to the yield strength (~0.9 f_y) and strains equal ε_s = 1.5‰. The results of the tests of deep beams with bent up bars DBII are presented in Table 1. Using the measured deformations, the forces in vertical reinforcement (F_v) and bent up bars (F_t), as well as the calculated on that bases force F_1 in the cantilever were determined. The last two columns of the table present the relation of force in vertical bars F_v to the force in the cantilever F_1, and the relation of the vertical component of bent up bars to the F_1 force.

In the two last lines of Table 1, the comparison of the F_1 force in the DBII deep beam obtained from the tests to the values coming from the design recommendations given by Leonhardt [14] and Schröeder [16] is presented.

The analysis of flow of force acting along the depth of the cantilever of the DBII deep beam based on the results of tests showed that the major portion of loading was taken over by bent up bars: about 0.6 F_1 considering all eight bars, and 0.54 F_1 for six bars, thus different from structural recommendations [14,16]. It is also worth mentioning that the share in taking over of vertical loading of the cantilever by lower diagonal bars, which did not cover the vertical suspended bars, was minor, which is proved by the measurement of steel deformation in gauge No. 8.

The S–T model for the analysis of the flow of forces in the cantilever deep beam loaded throughout the depth was also adopted by [24]. Fig. 12 shows a scheme of forces, that in contrast to the recommendations by Leonhardt's the suspended vertical reinforcement instead of force $0.6F_1$ is assigned a force equal $0.5F_1$, and diagonal bars should take over a force equal $0.5F_1/\cos\theta$.

In the analysis of S–T for the issue of load capacity of concrete compression struts at the time of occurring the inclined crack the stresses are not reaching the limit value of an uniaxial strain state. This issue was analyzed by Nielsen [25], Warwick and Foster [26],

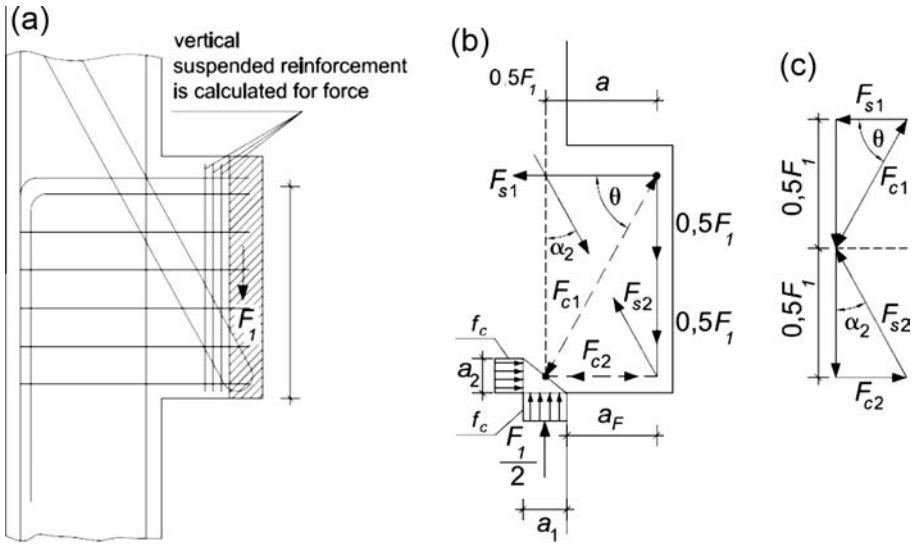

Fig. 12. Strut-and-Tie models for corbels loaded throughout the depth: (a) scheme of the reinforcement, (b) and (c) flow of forces [24].

Zhang and Hsu [27] and Collins and Mitchell [28] by introducing appropriate softening coefficient β reducing the uniaxial compression strength f_c.

Softening coefficient adopted in accordance with [25] is

$$\beta = 0.8 - \frac{f_c}{200}, \tag{5}$$

according to [26] where the impact of a_F/d is taking into account

$$\beta = 0.53 - \frac{f_c}{500} \quad \text{for } \frac{a_F}{d} \geqslant 2, \tag{6}$$

according to [27]

$$\beta = \frac{5.8}{\sqrt{f_c}} \cdot \frac{1}{\sqrt{1 + 400 \cdot \varepsilon_{ct}}} \leqslant \frac{0.9}{\sqrt{1 + 400 \cdot \varepsilon_{ct}}}, \tag{7}$$

according to [28], [29]

$$\beta = \frac{1}{1.14 + \left(0.64 + \frac{f_c}{470}\right) \cdot \left(\frac{a_F}{d}\right)^2}, \tag{8}$$

according to [1]

$$\beta = 0.6\left(1 - \frac{f_c}{250}\right). \tag{9}$$

Table 2 shows the comparison of softening coefficient β for the cantilever deep beam calculated on the basis of mentioned above assumptions and obtained from experimental tests based on the measurement of strains of inclined concrete compression strut. The maximum compression strains of the DBI were equal $\varepsilon_c = 1.24‰$ ($\sigma_c = 35.17$ MPa) and the DBII $\varepsilon_c = 0.65‰$ ($\sigma_c = 21.05$ MPa), while the average strains on the basis of the measurements and in accordance with the crack pattern $\varepsilon_c = 0.54‰$ ($\sigma_c = 17.48$ MPa) for DBI and $\varepsilon_c = 0.37‰$ ($\sigma_c = 12.67$ MPa) for the DBII.

For the cantilever deep beam DBI orthogonally reinforced, the softening coefficient can be estimated with sufficient accuracy for the area of concrete maximum effort according to the Collins and Vecchio analysis. While the best approximation formulas in the case of medium-strain analysis are specified by EC2 and by Warwick and Foster (in spite of the assumed shear slenderness $a_F/d \geqslant 2$).

In the cantilever deep beam DBII we can observed a clear decrease of the maximum strains of inclined concrete struts which may confirm a significant importance of the suitably shaped reinforcement in taking tensile stresses after the cracking. The low values of the strength reduction coefficient for concrete in the main strut for simply supported deep beams was provided by Matamoros and Wong [30] and it was equal 0.35.

Table 2
Comparison of softening coefficients in cantilever deep beams.

Type of analysis	Deep beam	Softening coefficient				
		β	$\beta_{exp,MAX}$[a]	$\beta_{exp,average}$[b]	$\beta_{exp,MAX}$[a]/β	$\beta_{exp,average}$[b]/β
Acc. to [25]	DBI	0.55	0.70	0.35	1.28	0.64
Acc. to [26]		0.43	0.70	0.35	1.64	0.81
Acc. to [27]		0.61	0.70	0.35	1.15	0.57
Acc. to [28]		0.77	0.70	0.35	0.91	0.45
Acc. to [1]		0.48	0.70	0.35	1.47	0.73
Acc. to [25]	DBII	0.55	0.42	0.25	0.77	0.46
Acc. to [26]		0.43	0.42	0.25	0.98	0.59
Acc. to [27]		0.61	0.42	0.25	0.69	0.41
Acc. to [28]		0.77	0.42	0.25	0.55	0.33
Acc. to [1]		0.48	0.42	0.25	0.88	0.53

[a] Softening coefficient according to the maximum compressive strains.
[b] Softening coefficient according to the average compressive strains.

Table 3
Comparison of failure forces obtained from experimental test and analysis of the Strut-and-Tie models [24].

Deep beam	Type of β analysis	Theoretical failure force (Fig. 12)									Experimental failure force			
		b (–)	θ (°)	$F_{c1,cal}$ (kN)	$\sigma_{c1,cal}$ (MPa)	$F_{s1,cal}$ (kN)	α (°)	$F_{c2,cal}$ (kN)	$\sigma_{c2,cal}$ (MPa)	$F_{s2,cal}$ (kN)	$F_{s1,exp}$ (kN)	$F_{s1,exp}/F_{s1}$ (–)	$F_{s2,exp}$ (kN)	$F_{s2,exp}/F_{s2}$ (–)
DBI	[25]	0.55	61.6	360.9	27.5	142.9	28.4	114.4	18.3	300.7	116.7	0.82	–	–
	[26]	0.43	61.4	301.4	21.5	144.4	28.6	144.4	21.5	301.4	116.7	0.81	–	–
	[27]	0.61	62.5	298.2	30.6	137.6	27.5	137.6	30.6	298.2	116.7	0.85	–	–
	[28]	0.77	63.1	296.8	38.5	134.4	26.9	134.4	38.5	296.8	116.7	0.87	–	–
	[1]	0.48	61.8	300.3	24.0	142.0	28.2	142.0	24.0	300.3	116.7	0.82	–	–
DBII	[25]	0.55	61.9	337.0	27.5	159.0	28.1	159.0	27.5	337.0	111.3	0.70	250.2	0.74
	[26]	0.43	60.9	340.1	21.5	165.4	29.1	165.4	21.5	340.1	111.3	0.67	250.2	0.74
	[27]	0.61	62.2	335.9	30.6	156.7	27.8	156.7	30.6	335.9	111.3	0.71	250.2	0.74
	[28]	0.77	62.8	334.1	38.5	152.7	27.2	152.7	38.5	334.1	111.3	0.73	250.2	0.75
	[1]	0.48	61.4	338.6	24.0	162.3	28.6	162.3	24.0	338.6	111.3	0.69	250.2	0.74

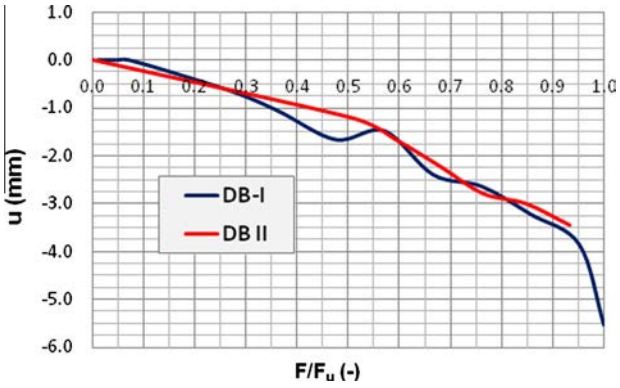

Fig. 13. Displacement of the bottom horizontal edge at the end of the cantilever of deep beams DBI and DBII.

From the calculated values of tensile forces (Table 3) in the horizontal reinforcement of the cantilever deep beam DBI, it follows that the theoretical forces (Fig. 12) obtained in terms of softening coefficient β according to [28] responds to the tension forces obtained from research with a sufficient compatibility. However, in the case of deep beam DBII accordance between the values of tensile forces using the S–T model and experimental research it is not so good. However, the next size of forces for horizontal and inclined reinforcement also obtained in accordance with [28].

The results of vertical displacements of the bottom edge of the cantilever of both tested deep beams are presented in Fig. 13. Comparing the maximum displacements of the deep beams, it may be noticed that in the DBII with additional bent up bars they were lower and came in the final stage of exhaustion the load capacity to 4.5 mm. While in the DBI with the orthogonal grid the displacements reached 5.5 mm.

5.2. The flow of forces in the transversal deep beam

In the transversal deep beam DBI, the strains in vertical stirrups, adopted from the $3t$ width was equal app. 0.75‰ (100 MPa) (Fig. 14). The strains in horizontal bars of the bottom reinforcement were equal app. 1.90‰ (400 MPa ~0.72 f_y).

During analyze of the results in the transversal deep beam of the DBII system it may be also concluded that the majority of tension stress was taken over by the bent up reinforcement in where the yielding was reached in one of the bars and ε_s = 1.25‰ (Fig. 15).

The stresses in the diagonal reinforcement suggest that the length of the anchoring bars have to retain the rule of bringing them to the vertical edge of the transversal deep beam with deflection on their ends.

In Table 4, similarly as in Table 1, the value of F_3 force in transversal deep beam of the DBII joint (Fig. 4) for: the vertical stirrups (F_v) adopted from the width $3t$ (12 ø8) and bent up bars F_t (12 ø12) is presented.

5.3. The cracking morphology and load carrying capacity

The crack pattern on the DBI and DBII deep beams surface at the final stage of load failure on the background of the trajectory of principal stresses is presented in Figs. 16 and 18. As it is noticeable, the cracking of the deep beam almost exactly corresponds to the direction of main compression stress determined using the FEM, assuming E_c = const.

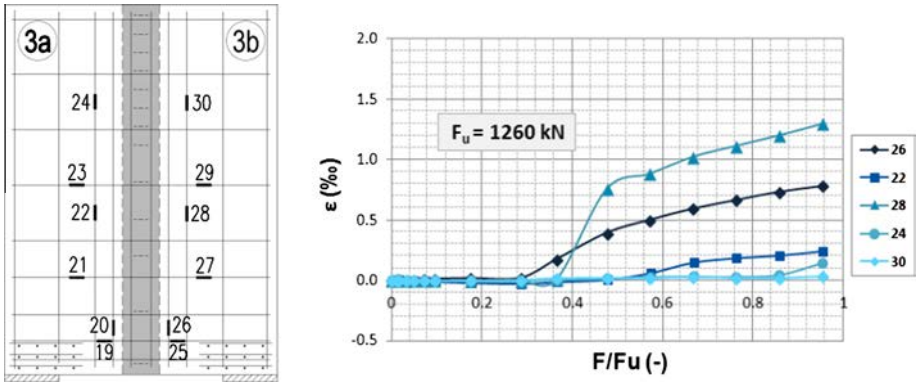

Fig. 14. Strains of the main reinforcement of the transversal deep beam of DBI with the vertical orthogonal reinforcement.

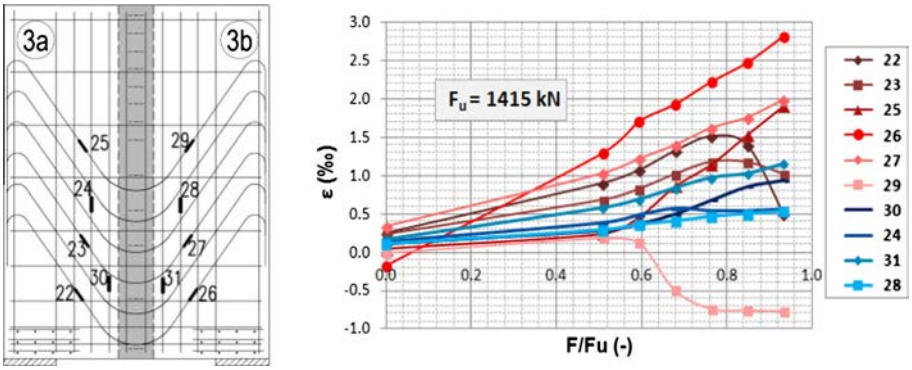

Fig. 15. Strains in the main reinforcement of the transversal deep beam of DBII system with additional bent up bars: in the vertical and diagonal reinforcement.

Table 4
Flow of force F_3 loading the transversal deep beam on the vertical reinforcement F_v and bent up one F_t.

Type of analysis	F_v (kN)	F_t (kN)	$F_t^* \sin a$ (kN)	F_3 (kN)	F_v/F (–)	$(F_t^* \sin a)/F_3$ (–)
From the exp. tests ($\sigma_{s,exp}$)	96.8	564.0	462.0	558.8	0.17	0.83
Assuming $\sigma_{s,exp} = f_y$	351.1	754.6	618.1	969.2	0.36	0.64
Failure force from statical analysis, $F = F_u = 1415$ kN	–	–	–	1301.8	–	–

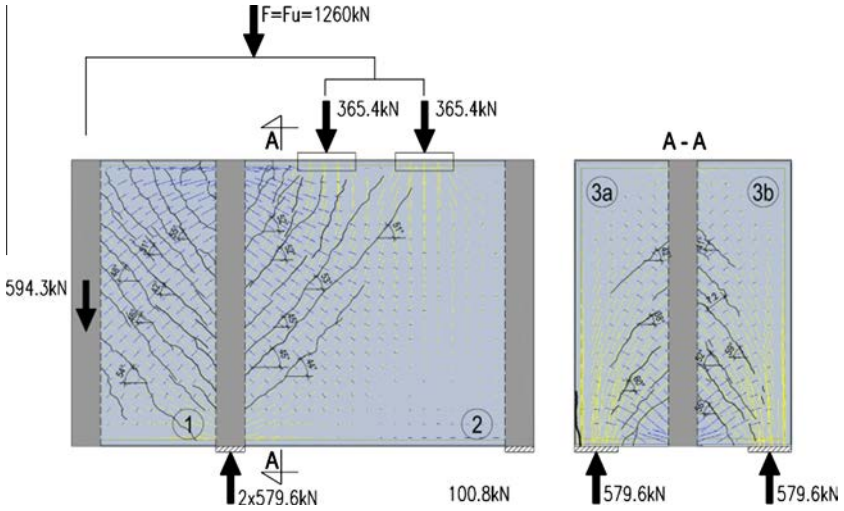

Fig. 16. DBI deep beam crack pattern on the background of the main stress trajectory, with the failure force $F_u = 1260$ kN.

In both tested deep beams, the first cracks emerged in the tensed upper corner of the cantilever at the joint with the transversal deep beam. The first crack of the DBI orthogonally reinforced appeared at the force $F = 357$ kN = $0.28F_u$ which determined the force F_1 of 150 kN = $0.28F_u$ on cantilever, while in the transversal deep beam DBI (3) the initial cracking force was 460 kN = 0.37 F_u ($F_3 = 442$ kN). The DBII deep beam with additional diagonal reinforcement cracked under the force of $F = 480$ kN = $0.34F_u$ which made the force on the cantilever $F_1 = 201$ kN. On the transversal deep beam, the first crack was observed in the total load of $F = 600$ kN which consisted of 0.42 F_u, while directly on the transversal beam that value was $F_3 = 576$ kN.

In the orthogonally reinforced deep beams (DBI) the width of crack was definitely higher compared to the additional diagonal reinforcement deep beam (DBII). At the failure of the DBI cantilever, the width of the crack was 0.24 mm, while for the diagonal reinforcement it was only 0.12 mm. In order to compare the width

Fig. 17. Crack pattern of DBI deep beam before failure.

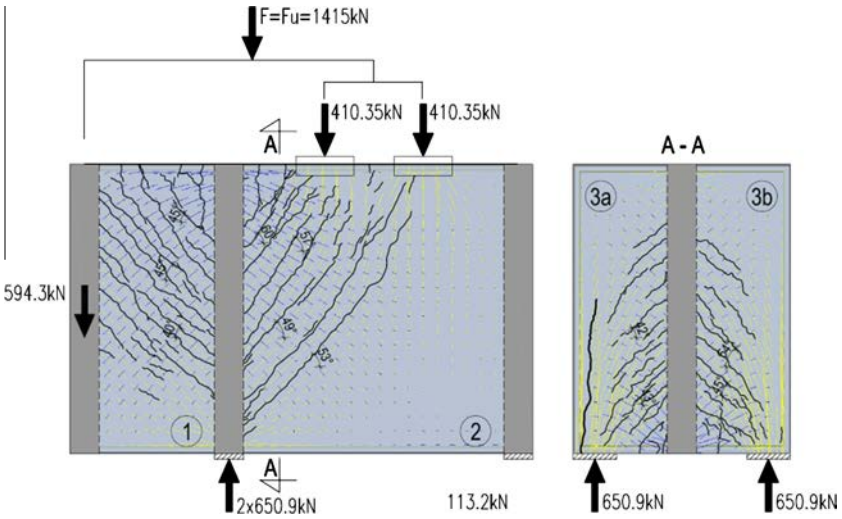

Fig. 18. DBII deep beam crack on the background of main stress trajectory, with the failure load F_u = 1415 kN.

Table 5
The cracking force and width of cracks in the DBI and DBII deep beams.

	Deep beam	F_{cr}[a] (kN)	Width of the cracks w_i (mm) for the designed load	
			Service ≈ $0.6F_{u,design}$	Failure $F_{u,design}$
DBI	Cantilever deep beam (1)	357	0.16	0.24
	Transversal deep beam (3)	460	0.12	0.28
DBII	Cantilever deep beam (1)	480	0.10	0.12
	Transversal deep beam (3)	600	0.04	0.10

[a] F_{cr} (kN) in reference to the total load F acting on the deep beam system.

of the cracks, in Table 5 the widths for the design load were shown: design service load of app. 60% of the failure load, and the failure load (F_u). In the transversal deep beam in the case of the DBII joint, the higher number of cracks whose width increased slower that it was shown for DBI. The favorable influence of the bent up bars on limitation of cracking was also proved by the tests of dapped-end beams with mixed reinforcement [18].

The photos of the tested specimens were presented in Figs. 17 and 19. The failure of both deep beams occurred through the destruction of the support area of the transversal beam and it was preceded by an abrupt emergency of crack in the support zone, running almost vertically. In the DBI deep beam, the failure crack appeared the force reached 1200 kN, just before the full load capacity was attained. The failure was abrupt.

Fig. 19. Crack pattern of DBII deep beam after failure.

The DBI deep beam was failured under the load of 1260 kN while the DBII under the 1415 kN load. Thus, both deep beams reached the designed load capacity of 1200 kN.

6. Conclusions

The load capacity of the DBII deep beam with the additional bent up bars occurred to be higher compared to the DBI reinforced with the orthogonal reinforcement, while the latter one excited only slightly the design value.

The diagonal reinforcement influenced also favorably on limitation of cracks width in the cantilever and transversal beams.

The strains in the bent up bars proved the effective performance of the reinforcement of bars crossing the pilaster through which the load was transmitted to the cantilever. In the lower bent up bars which did not meet that requirement the stresses were low.

As it occurred from the carried out research (as it was in the tested spatial deep beam [15]) the results are dependent on the geometry of the deep beam spatial system, as well as on the way of load transmission and arrangement of reinforcement. It is particularly important for the design of cantilever deep beams.

In analyzed case, for orthogonally reinforced cantilever deep beam DBI, the softening coefficient can be estimated with sufficient accuracy for the area of maximum concrete effort according to the [28]. While the best approximation formulas in the case of medium-strain analysis are specified by EC2 and by [26].

In the cantilever deep beam DBII we can observe a clear decrease of maximum strains of concrete diagonals which may confirm an significant importance of suitably shaped reinforcement in taking tensile stresses after the cracking.

It is necessary to modify the Strut-and-Tie model for cantilever deep beam loaded throughout the depth and taking into account

the variable shear slenderness for better accordance softening coefficient and the flow of forces in the reinforcement.

Therefore, it can be concluded that in order to specify formulas of dimensioning of reinforced deep beams including cantilever specimens further tests are necessary.

References

[1] EN 1992-1-1. Eurokod 2: design of concrete structure, part 1 – general rules and rules for buildings; 2004. p. 225.
[2] ACI Standard Code 318M-08. Building code requirements for reinforced concrete and commentary. American Concrete Institute; 2008. p. 473.
[3] MC2010 – fib Model Code for Concrete Structures 2010. Berlin: Ernst und Sohn; 2013. p. 402.
[4] Kong FK, Robins PJ, Cole DF. Web reinforcement effects on deep beams. ACI J Pro 1970;67(12):1010–7.
[5] Rogowsky DM, MacGregor JG, Ong SY. Tests of reinforced concrete deep beams. ACI J Pro 1986;83(4):614–23.
[6] Ulańska D. Badania doświadczalne elementów i konstrukcji betonowych. Politechnika Łódzka: Wydawnictwo Katedry Budownictwa Betonowego, Zeszyt 1; 1991, Łódź:45–99 [in Polish].
[7] Godycki-Ćwirko T. Wandartige Stahlbetonträger mit Auflagerverstärkungen (Lisenen) im Zustand I und II. Bauplannung-Bautechnik, 23 Jg., Heft 6 Juni 1969:291–5 und Heft 7 Juli 1969:345–6 [in German].
[8] Birrcher DB, Tuchscherer RG, Huizinga M, Bayrak O. Minimum web reinforcement in deep beams. ACI Struct J 2013;110(2):297–306.
[9] Tan KH, Kong FK, Teng S, Weng LW. Effect of web reinforcement on high-strength concrete deep beams. ACI Struct J 1997;94(5):572–82.
[10] Yang KH, Chung HS, Lee ET, Eun HC. Shear characteristics of high-strength concrete deep beams without shear reinforcements. Eng Struct 2003;25:1343–52.
[11] Birrcher DB, Tuchscherer RG, Huizinga M, Bayrak O. Depth effect in deep beams. ACI Struct J 2014;111(4):731–40.
[12] Zhang N, Tan KH. Direct strut-and-tie model for single span and continuous deep beams. Eng Struct 2007;29:2987–3001.
[13] Foster SJ, Gilbert RI. Experimental studies on high-strength concrete deep beams. ACI Struct J 1998;95(4):382–90.
[14] Leonhardt F, Mönnig E. Vorlesungen über Massivbau. Berlin: Dritter Teil, Springer-Verlag; 1974. p. 175–80 [in German].
[15] Leonhardt F, Walther R. Wandartige Träger. Deutscher Ausschuss für Stahlbeton, nr 178; 1966. p. 159 [in German].
[16] Schröder K. Berechnung und Konstruktion wandartiger Träger und Kragscheiben im Stahlbetonbau. Bauplannung-Bautechnik, 36 Jg., Heft 6 Juni 1982. p. 274 [in German].
[17] Nagrodzka-Godycka K, Knut A, Zmuda-Baszczyn K. Żelbetowy wspornik węzła tarczowego obciążony wzdłuż krawędzi pionowej. Inżynieria Morska i Geotechnika 2014;5:504–12 [in Polish].
[18] Nagrodzka-Godycka K, Piotrkowski P. Experimental study of dapped-end beams subjected to inclined load. ACI Struct J 2012;109(1):11–20.
[19] Park J, Kuchma D. Strut-and-Tie model analysis for strength prediction of deep beams. ACI Struct J 2007;104(6):657–66.
[20] Matamoros AB, Wong KH. Design of simply supported deep beams using Strut-and Tie models. ACI Struct J 2003;100(6):704–12.
[21] Hwang SJ, Lu WY, Lee HJ. Shear strength prediction for deep beams. ACI Struct J 2000;97(3):367–76.
[22] Muttoni A, Ruiz MF, Niketić F. Design versus assessment of concrete structures using stress fields and Strut-and-Tie models. ACI Struct J 2015;112(5):605–16.
[23] Amini Najafian H, Vollum RL, Fang L. Comparative assessment of finite-element and strut and tie based design methods for deep beams. Mag Concr Res 2013;65(16):970–86.
[24] Nagrodzka-Godycka K. Wsporniki żelbetowe. Badania, teoria, projektowanie. Monografia nr 21. Wydawnictwo Politechniki Gdańskiej, Gdańsk; 2001 [in Polish].
[25] Nielsen MP, Braestrup MW, Jensen BF, Bach F. Concrete Plasticity, Beam-Shear in Joints, Punching Shear, Publ. of the Danish Soc. for Struct. Scien. and Eng. T. U. Lyngby, Copenhagen, Denmark, nr 129; 1978.
[26] Warwick WB, Foster SJ. Investigation into the efficiency factor used in nonflexural reinforced concrete member design, UNICIV Report R – 320. Univ. of New South Wales; July 1993.
[27] Zhang LXB, Hsu TTC. Behavior and analysis of 100 MPa concrete membrane elements. J Struct Eng ASCE 1998;124(1).
[28] Collins MP, Mitchell D. A rational approach to shear design. ACI J Pro 1986;83 (6):925–33.
[29] Foster SJ, Gilbert RJ. The design of nonflexural members with normal and high-strength concrets. ACI J Pro 1996;93(1):3–10.
[30] Matamoros AB, Wong KH. Design of simply supported deep beams using Strut-and-Tie models. ACI Struct J 2003;100(6):704–12.